Multiscale recrystallization models for the prediction of crystallographic textures with respect to process simulation

D Raabe
Max–Planck–Institut für Eisenforschung, Max–Planck–Str. 1, Düsseldorf, 40237, Germany. email: raabe@mpie.de

The manuscript was received on 17 March 2006 and was accepted after revision for publication on 15 November 2006.

DOI: 10.1243/03093247JSA219

Abstract: This paper discusses the most relevant multiscale models for predicting crystallographic textures formed during the primary static recrystallization of metals. Two main groups of approaches are presented, namely those which spatially discretize the grains and the interface motion associated with recrystallization and those which treat these phenomena in an Avrami-type statistical fashion. The article gives a concise review of the methods, placing particular attention on their strengths and weaknesses in the context of process modelling, of conceptual aspects, and of the data sets required as input for practically applying the models to the prediction of crystallographic textures in the course of metallurgical processes.

Keywords: simulation, cellular automata, Potts model, Monte Carlo methods, recrystallization, Avrami model, nucleation, crystal plasticity, grain growth, grain boundary

1 RECRYSTALLIZATION MODELS FOR PROCESS SIMULATION

The use of models for describing recrystallization phenomena with the aim of predicting crystallographic texture, microstructure, and mechanical properties in the context of materials processing is a challenging task [**1**–**6**]. This judgement is motivated by the common observation that substantial changes in recrystallization phenomena can be stimulated by rather small modifications in the metallurgical state (e.g. chemical purity, thermodynamic state, crystallographic texture, microstructure inhomogeneity, and microstructure inheritance from preceding process steps) or in the external boundary conditions (time, temperature fields, strain fields, and joint thermal and mechanical constraints) [**7**–**9**]. This sensitivity of recrystallization arises because most of the metallurgical mechanisms involved during texture formation in the course of recrystallization such as grain nucleation, grain boundary mobility, or impurity drag effects are thermally activated. Typically these mechanisms follow exponential functions the arguments of which may depend on some of the parameters listed above and interact with each other in a non-linear fashion. Similarly, the microstructural state of the deformed material from which recrystallization proceeds is often not well known or not well reproduced in models. Although various types of homogenization model of crystal deformation are nowadays capable of providing a decent picture of the average behaviour of the material in the course of a thermomechanical process, often the details and inhomogeneities in the deformed structure that strongly affect recrystallization are unknown so that even a good knowledge of averages does not generally solve the open questions pending in the field of recrystallization modelling.

Moreover, in real industrial materials manufacturing processes typically encountered in physical metallurgy, many of the influencing factors, be they of a metallurgical or of a processing nature, are usually not exactly known nor sufficiently well defined to apply models which require a high degree of precision with regard to the input parameters.

These remarks emphasize that the selection of an appropriate recrystallization multiscale model for the prediction of crystallographic texture, microstructure, and properties for a given process must follow a clear concept as to what exactly is expected from such a model and what cannot be predicted by it in view of the points made above. This applies in particular

to cases where a model for the simulation of recrystallization textures is to be used in conjunction with real manufacturing processes [**10**].

The main challenge of using multiscale process models for recrystallization, therefore, lies in selecting the right model for a well-defined task, i.e. it must be agreed which microstructural property is to be simulated and what kind of properties should be subsequently calculated from these microstructure data. From that it is obvious that no model exists which could satisfy all questions that may arise in the context of recrystallization textures. Also the aims of predicting recrystallization textures and microstructures on the one hand and the materials properties (functional or mechanical) on the other have to be clearly separated. While the first task may by pursued by formulating an appropriate recrystallization model within the limits addressed above, the second challenge falls into the wide realm of microstructure–property theory. This means that generally the prediction of the microstructure and the prediction of some property from that particular microstructure should be separated. Typically through-process modellers are interested in the final materials properties in the first place rather than in the details of the microstructure of a recrystallized material. The modern attitude towards this discrepancy is the commonly accepted understanding that a decent description of materials properties requires the use of internal (i.e. of microstructurally motivated) parameters which can be coupled to suitable microstructure–property laws. A typical example along those philosophy lines would be the grain size prediction via a recrystallization model and the subsequent application of the Hall–Petch law for the estimation of the yield strength.

This article addresses exclusively the first question and, more precisely, only models for primary static recrystallization will be tackled, placing particular attention on the simulation of crystallographic textures. To be more specific the plan of this article is as follows. In the first part following this introduction, some spatially discrete recrystallization models are introduced and concisely discussed with respect to their particular capability to serve in through-process models for the simulation of crystallographic textures. The second part presents a discussion of recrystallization models for texture prediction which treat these phenomena in a statistical Avrami-type fashion. The discussion reviews the strengths and weaknesses of the different approaches in the context of process modelling, of multiscale aspects, of conceptual challenges, and of the data sets required as input to apply these models practically for process simulation in an actual manufacturing environment. In order to avoid repetition of equations which have been presented in many earlier publications on the various models addressed, the current study aims at presenting the material without mathematical derivations but rather with the aim of focusing on the basic philosophy behind the various models, with respect to the prediction of crystallographic textures in the context of process modelling.

2 SPATIALLY DISCRETE MODELS FOR PREDICTING RECRYSTALLIZATION TEXTURES

2.1 Introduction

The design of time- and space-discretized recrystallization models for predicting texture and microstructure in the course of materials processing which track kinetics and energies in a local fashion are of interest for two reasons. First, from a fundamental point of view it is desirable to understand better the dynamics and the topology of microstructures that arise from the interaction of large numbers of lattice defects which are characterized by a wide spectrum of intrinsic properties and interactions in spatially heterogeneous materials under complex engineering boundary conditions. For instance, in the field of recrystallization (and grain growth) the influence of local grain boundary characteristics (mobility and energy), local driving forces, and local crystallographic textures on the final microstructure is of particular interest. An important point of interest in that context, however, is the question of how local such a model should be in its spatial discretization in order really to provide microstructural input that cannot be equivalently provided by statistical methods. In the worst case a problem in that field may be that spatially discrete recrystallization models may have the tendency to pretend a high degree of precision without actually providing it. In other words, even in highly discretized recrystallization models the physics always lies in the details of the constitutive description of the kinetics and thermodynamics of the deformation structure and of the interfaces involved. The mere fact that a model is formulated in a discrete fashion does not, as a rule, automatically render it a sophisticated model *per se*. Second, from a practical point of view it makes sense to predict microstructure parameters such as the crystal size or the crystallographic texture which determine the mechanical and physical properties of materials subjected to industrial processes on a sound phenomenological basis.

In this part of the study on spatially discrete models, particular attention is paid to cellular automata, Potts-type Monte Carlo multispin models, and vertex (front-tracking) models because those three have been used in the past for the simulation of recrystallization textures with respect to process design. Related spatially discrete models of recrystallization phenomena such as the phase field model as the metallurgically motivated derivative of the Ginzburg–Landau kinetic theory represent of course highly capable and elegant ways to predict the evolution of topology during recrystallization but they have been up to now less prominent for predicting crystallographic textures during recrystallization and will, therefore, not be discussed in this report. A related excellent overview article on the modelling of grain coarsening and recrystallization phenomena has been published earlier by Miodownik [**11**].

2.2 Cellular automaton models of recrystallization

Cellular automata are algorithms that describe the discrete spatial and temporal evolution of complex systems by applying local transformation rules to lattice cells which typically represent volume portions [**12**]. The state of each lattice site is characterized in terms of a set of internal state variables. For recrystallization models these can be lattice defect quantities (stored energy), crystal orientation, or precipitation density. Each site assumes one out of a finite set of possible discrete states. The opening state of the automaton is defined by mapping the initial distribution of the values of the chosen state variables on to the lattice.

The dynamic evolution of the automaton takes place through the application of deterministic or probabilistic transformation rules (switching rules) that act on the state of each lattice point. These rules determine the state of a lattice point as a function of its previous state and the state of the neighbouring sites. The number, arrangement, and range of the neighbouring sites used by the transformation rule for calculating a state switch determines the range of the interaction and the local shape of the areas which evolve. Cellular automata work in discrete time steps. After each time interval the values of the state variables are updated for all points in synchrony mapping the new (or unchanged) values assigned to them through the transformation rule. Owing to these features, cellular automata provide a discrete method of simulating the evolution of complex dynamic systems which contain large numbers of similar components on the basis of their local interactions. A more formal description of the basics of cellular automata for microstructure modelling has been given in reference [**12**] and previous applications in the field of recrystallization and recovery have been discussed in references [**13**] to [**22**].

Cellular automata are, like all other continuum models that work above the discrete atomic scale, not intrinsically calibrated by a characteristic physical length scale or timescale. This means that a cellular automaton simulation of continuum systems requires the definition of elementary units and transformation rules that adequately reflect the kinetics at the level addressed. If some of the transformation rules refer to different real timescales (e.g. recrystallization and recovery, bulk diffusion, and grain boundary diffusion) it is essential to achieve a correct common scaling of the entire system [**3**, **6**, **22**–**29**]. The requirement for an adjustment of time scaling among various rules arises because the transformation behaviour of a cellular automaton is sometimes determined by non-coupled Boolean routines rather than by local solutions of coupled differential equations.

The following examples on the use of cellular automata for predicting recrystallization textures are designed as automata with a probabilistic transformation rule [**22**–**29**]. Independent variables are time and space. The latter is discretized into equally shaped cells each of which is characterized in terms of the mechanical driving force (stored deformation energy) and the crystal orientation (texture). The starting data of such automata are usually derived from experiment (for instance from a microtexture map) or from plasticity theory (for instance from crystal plasticity finite element simulations). The initial state is typically defined in terms of the distribution of the crystal orientation and of the driving force. Grains or subgrains are mapped as regions of identical crystal orientation, but the driving force may vary inside these areas.

The kinetics of the automaton result from changes in the state of the cells (cell switches). They occur in accord with a switching rule (transformation rule) which determines the individual switching probability of each cell as a function of its previous state and the state of its neighbouring cells. The switching rule is designed to map the phenomenology of primary static recrystallization. It reflects the fact that the state of a non-recrystallized cell belonging to a deformed grain may change owing to the expansion of a recrystallizing neighbouring grain which grows according to the local driving force and boundary mobility. If such an expanding grain sweeps a non-recrystallized

cell, the stored dislocation energy of that cell drops to zero and a new orientation is assigned to it, namely that of the expanding neighbouring grain. The mathematical formulation of the automaton used in this report can be found in references [**22**] to [**29**]. It is derived from a probabilistic form of a linearized symmetric rate equation, which describes grain boundary motion in terms of isotropic single-atom diffusion processes perpendicular through a homogeneous planar grain boundary segment under the influence of a decrease in the Gibbs energy. This means that the local progress in recrystallization can be formulated as a function of the local driving forces (stored deformation energy) and interface properties (grain boundary mobility). The most intricate point in such simulations consists in identifying an appropriate phenomenological rule for nucleation events.

Figure 1 shows the kinetics and some three-dimensional microstructures sketches, of a recrystallizing aluminum sample which had an initial dislocation density of $10^{15}\,\mathrm{m}^{-2}$ [**22**]. The simulation used site-saturated nucleation conditions, i.e. the nuclei were at $t = 05$ s statistically distributed in physical space and orientation space. The grid size was $10\,\mu\mathrm{m} \times 10\,\mu\mathrm{m} \times 10\,\mu\mathrm{m}$. The cell size was 0.1 μm. All grain boundaries had the same mobility using an activation energy of the grain boundary mobility of 1.3 eV and a pre-exponential factor of the boundary mobility of $m_0 = 6.2 \times 10^{-6}\,\mathrm{m}^3/\mathrm{N\,s}$. Small-angle grain boundaries had a mobility of zero. The temperature was 800 K. The time constant of the simulation was 0.35 s.

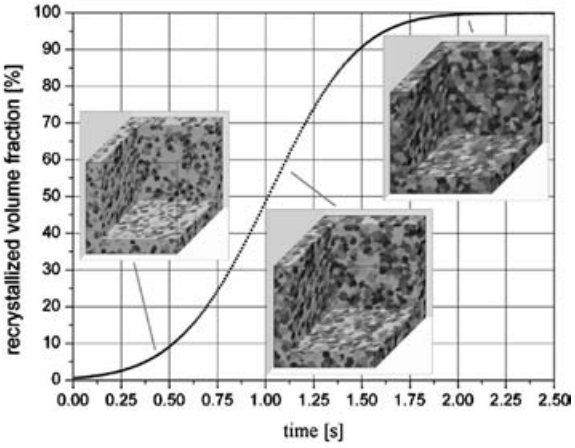

Fig. 1 Kinetics and microstructure of recrystallization in a plastically strained aluminium single crystal. The deformed crystal had a (011)[100] orientation and a uniform dislocation density of $10^{15}\,\mathrm{m}^{-2}$; site-saturated nucleation conditions at 800 K [**21**]

Figure 2 shows an example of a coupling of a cellular automaton with a crystal plasticity finite element model for predicting recrystallization textures in aluminium [**26**]. The major advantage of such an approach, when compared with the example shown in Fig. 1, is that it considers the inherited material deformation heterogeneity as opposed to material homogeneity that was assumed in Fig. 1.

This type of coupling the two models, therefore, seems more appropriate when aiming at the simulation of textures formed during materials processing. Nucleation in this coupled simulation works above the subgrain scale, i.e. it does not explicitly describe cell walls and subgrain coarsening phenomena. Instead, it incorporates nucleation on a more phenomenological basis using the kinetic and thermodynamic instability criteria known from classical recrystallization theory [**7**–**9**]. The kinetic instability criterion means that a successful nucleation process leads to the formation of a mobile large-angle grain boundary which can sweep the surrounding deformed matrix. The thermodynamic instability criterion means that the stored energy changes across the newly formed large-angle grain boundary, providing a net driving force that pushes it forwards into the deformed matter. Nucleation in this simulation is performed in accord with these two aspects, i.e. potential nucleation sites must fulfil both the kinetic and the thermodynamic instability criteria. The used nucleation model does not create any new orientations. At the beginning of the simulation the thermodynamic criterion, i.e. the local value of the dislocation density, was first checked for all lattice points. If the dislocation density was larger than some critical value of its maximum value in the sample, the cell was spontaneously recrystallized without any orientation change, i.e. a dislocation density of zero was assigned to it and the original crystal orientation was preserved. In the next step the conventional cellular growth algorithm was used, i.e. the kinetic conditions for nucleation were checked by calculating the misorientations among all spontaneously recrystallized cells (preserving their original crystal orientation) and their immediate neighbourhood considering the first-, second-, and third-neighbour shells. If any such pair of cells revealed a misorientation above 15°, the cell flip of the unrecrystallized cell was calculated according to its actual transformation probability. In the case of a successful cell flip the orientation of the first-recrystallized neighbour cell was assigned to the flipped cell.

Figures 3 and 4 show a two-dimensional cellular automaton simulation of the recrystallization texture

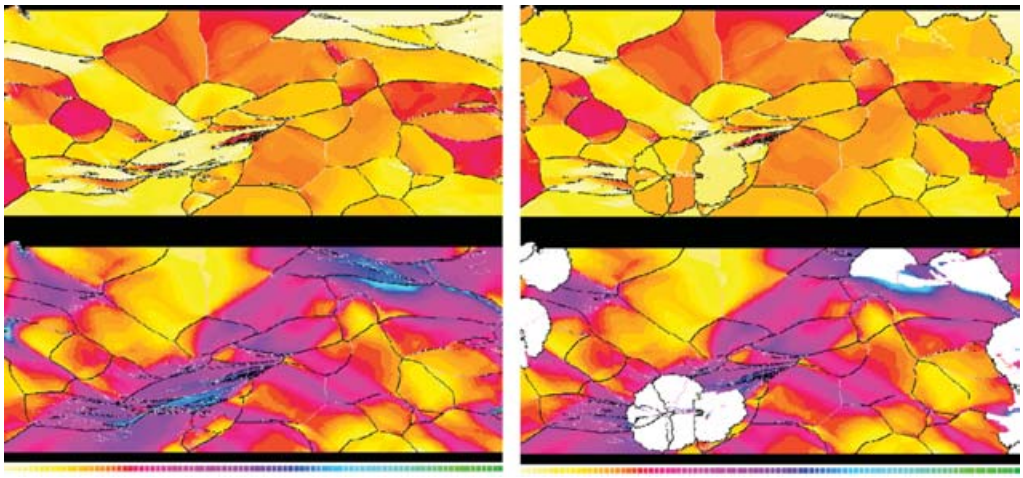

Fig. 2 Two-dimensional simulation of recrystallization in aluminium on the basis of crystal plasticity finite element starting data. The lower micrographs show the change in dislocation density; the upper micrographs show the texture in terms of the magnitude of the Rodriguez vector. The white areas in the two lower figures indicate a stored dislocation density of zero, i.e. these areas are recrystallized. The simulation parameters are as follows: 800 K; site-saturated spontaneous nucleation in cells with at least 50 per cent of the maximum occurring dislocation density; growth misorientations above 15° at an activation energy of the grain boundary mobility of 1.46 eV and a pre-exponential factor of the grain boundary mobility of $m_0 = 8.3 \times 10^{-3}$ m^3/N s. See details in reference [**25**]

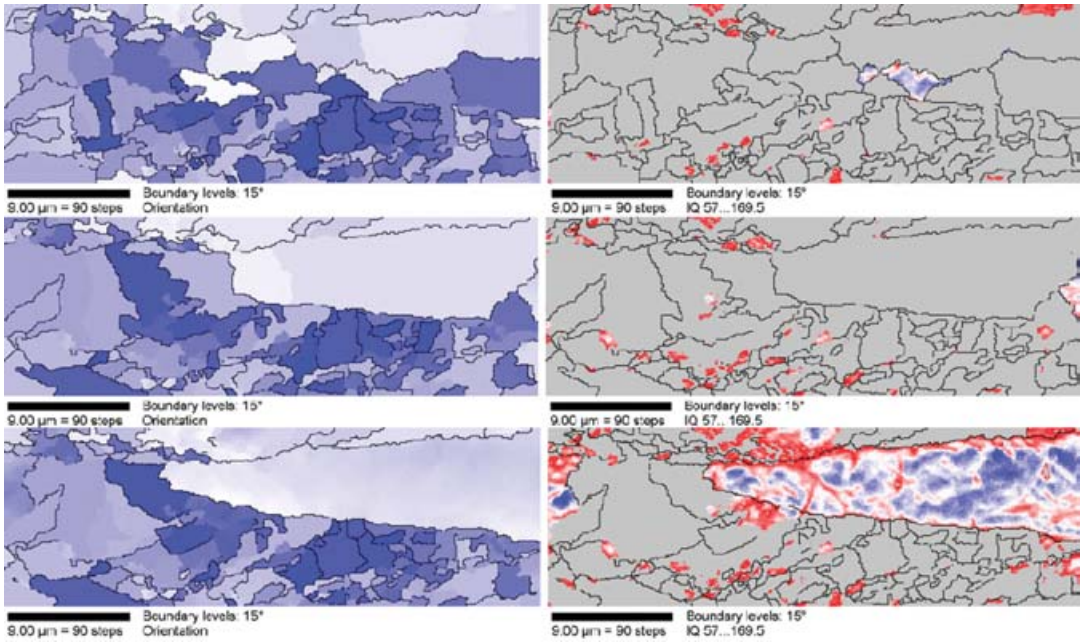

Fig. 3 Set of simulated microstructures for different values of the precipitated volume fractions f of foreign precipitates in an recrystallized IF steel ($f = 28$ per cent, 29 per cent, and 30 per cent from the top to the bottom). The nucleation criterion was that all cells with a dislocation density above 80 per cent of the occurring maximum value undergo spontaneous recrystallization at $t = 0$ s (i.e. a critical dislocation density greater than $> 37.6 \times 10^{14}$ m^{-2}); classical Zener pinning. The left-hand side figures are the texture maps; the right hand side figures are the dislocation density map (the grey colour indicates the fully recrystallized state). Details of this simulation have been given in reference [**28**]

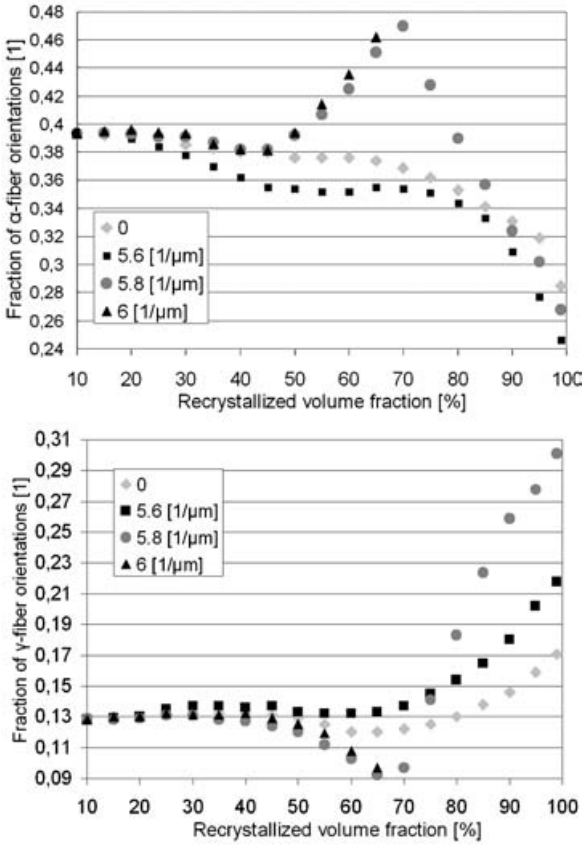

Fig. 4 Evolution of the crystallographic texture of the simulation shown in Fig. 3 for a recrystallized IF steel in terms of the α-fibre and the γ-fibre during the simulated annealing when considering the particle drag for different ratios of the volume fraction to the particle radius [**28**]. f is the precipitated volume fractions of second-phase particles

of a 75 per cent cold-rolled interstitial-free (IF) sheet steel under consideration of Zener particle pinning [**29**]. The model is applied to experimentally obtained high-resolution microtexture electron backscattered diffraction (EBSD) data. The simulation is discrete in time and space. Orientation is treated as a continuous variable in Euler space. The dislocation density distribution is approximated from the Kikuchi pattern quality of the experimental EBSD data. It is used for the calculation of the scalar driving force field required for the recrystallization simulation. Different submodels for nucleation and for the influence of Zener-type particle pinning were tested. Figure 3 shows an approximation obtained by using the classical Zener formulation [**7**–**9**]. Real-time and space calibration of the simulation is obtained by using experimental input data for the grain boundary mobility, the driving forces, and the length scale of the deformed microstructure as mapped by the high-resolution EBSD experiments. The simulations predict the kinetics and the evolution of microstructure and texture during primary static recrystallization. Depending on the ratio of the precipitated volume fraction and the average radius of the particles the simulations reveal three different regimes for the influence of particle pinning on the resulting microstructures, kinetics, and crystallographic textures.

2.3 Potts-type Monte Carlo multispin models of recrystallization

The application of the Metropolis Monte Carlo method in microstructure simulation has gained momentum particularly through the extension of the Ising lattice model for modelling magnetic spin systems to the kinetic multistate Potts lattice model [**3**, **6**, **30**–**36**]. The original Ising model is in the form of an $\frac{1}{2}$ spin lattice model where the internal energy of a magnetic system is calculated as the sum of pair interaction energies between the continuum units which are attached to the nodes of a regular lattice. The Potts model deviates from the Ising model by generalizing the spin and by using a different Hamiltonian. It replaces the Boolean spin variable where only two states are admissible (spin up and spin down) by a generalized variable which can assume one out of a larger spectrum of discrete possible ground states and accounts only for the interaction between dissimilar neighbours. The introduction of such a spectrum of different possible spins enables domains to be represented discretely by regions of identical state (spin). For instance, in microstructure simulation such domains can be interpreted as areas of similarly oriented crystalline matter. Each of these spin orientation variables can be equipped with a set of characteristic state variable values quantifying the lattice energy, the dislocation density, the Taylor factor, or any other orientation-dependent constitutive quantity of interest. Lattice regions which consist of domains with identical spins or states are in such models translated as crystal grains. The values of the state variable enter the Hamiltonian of the Potts model. The most characteristic property of the energy operator when used for coarsening models is that it defines the interaction energy between nodes with like spins to be zero, and between nodes with unlike spins to be one. This rule makes it possible to identify interfaces and to quantify their energy as a function of the abutting domains.

The Potts model is very versatile for describing coarsening phenomena. It takes a quasi-microscopic metallurgical view of grain growth or ripening, where the crystal interior is composed of lattice points (e.g. atom clusters) with identical energies (e.g. orientations) and the grain boundaries are the interfaces between the different types of these domains. As in a real ripening scenario, interface curvature leads to increased wall energy on the convex side and thus to wall migration entailing local shrinkage. The discrete simulation steps in the Potts model, by which the system proceeds towards thermodynamic equilibrium, are typically calculated by randomly switching lattice sites and weighting the resulting interfacial energy changes in terms of Metropolis Monte Carlo sampling. Microstructure simulations using the Potts model have been devoted to recrystallization and grain growth [**3**, **6**, **30**–**36**].

Figures 5 and 6 shows two examples of Potts-type Monte Carlo models for predicting recrystallization textures. The example presented in Fig. 5 is a Potts Monte Carlo simulation of subgrain coarsening applied to orientation data of a low-carbon steel obtained from transmission electron microscopy orientation measurements inside a single grain. Details on this simulation have been given in references [**37**] and [**38**]. Figure 6 shows Potts Monte Carlo simulations of grain and subgrain coarsening applied to subgrain orientation data of a low-carbon steel obtained from high-resolution EBSD orientation measurements obtained inside a small group of deformed grains [**37**, **38**].

2.4 Vertex models of recrystallization

Vertex and related front-tracking simulations are another alternative for engineering process models with respect to recrystallization phenomena. Their use is currently less common when compared with the widespread application of Monte Carlo and cellular automaton models owing to their geometrical complexity and the required small integration time steps. Despite these differences from the lattice-based models they have an enormous potential for predicting interface dynamics on small scales also in the context of process simulations [**11**, **39**–**51**].

Topological network and vertex models idealize solid materials or soap-like structures as homogeneous continua which contain interconnected boundary segments that meet at vertices, i.e. boundary junctions. Depending on whether the system dynamics lie in the motion of the junctions or of the boundary segments, they are sometimes also referred to as boundary dynamics or, more generalized, as front-tracking models. The grain boundaries appear as lines or line segments in two-dimensional simulations, and as planes or planar segments in three-dimensional simulations. The dynamics of these coupled interfaces or interface portions and of the vertices determine the evolution of the entire network.

The dynamic equations of the boundary and node (vertex) motion can be described in terms of a damped Newtonian equation of motion which contains a large frictional portion or, mathematically equivalent, in terms of a linearized first-order rate

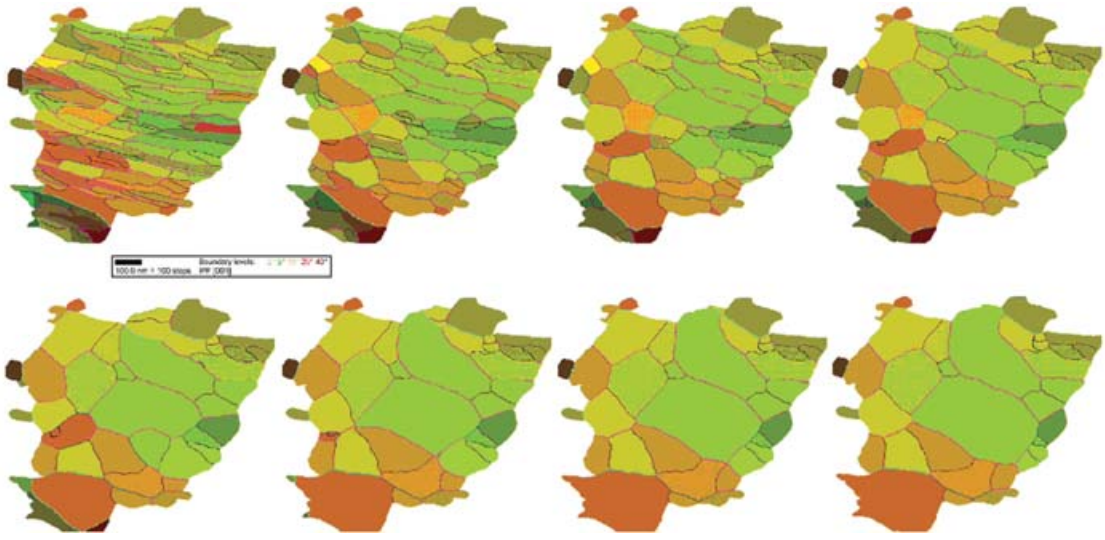

Fig. 5 Potts-type Monte Carlo simulation of subgrain coarsening applied to orientation data of a low-carbon steel obtained from transmission electron microscopy orientation measurements inside a single deformed grain. Details on this simulation have been given in references [**36**] and [**37**]. The colour code indicates the grain orientation in terms of one Miller triple

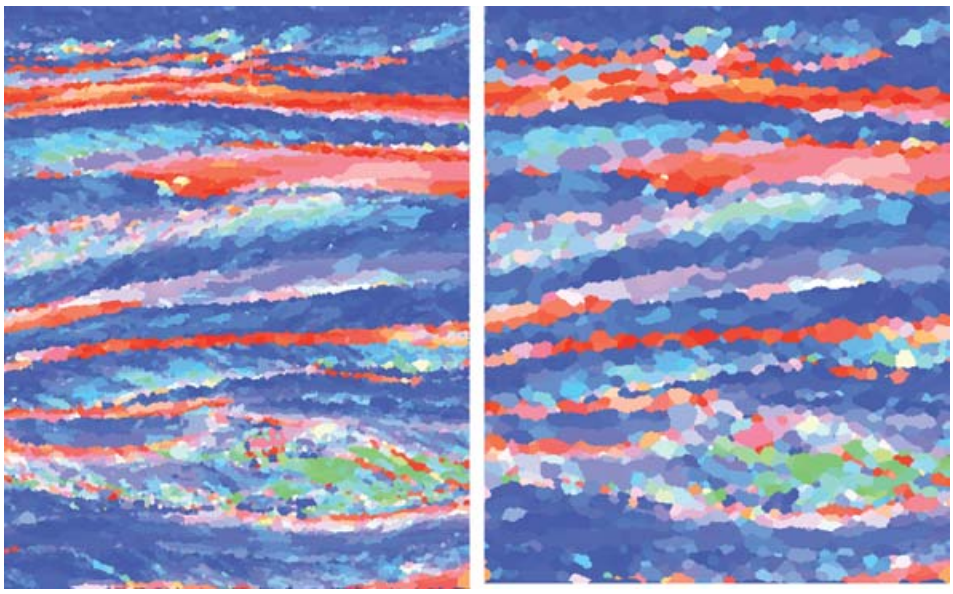

Fig. 6 Potts-type Monte Carlo simulation of grain- and subgrain-coarsening phenomena applied to subgrain orientation data of a low-carbon steel obtained from EBSD orientation measurements inside a small group of deformed grains. Details on the EBSD data and on the simulation have been given in references [**36**] to [**38**]. The colour code indicates the affiliation with one of the main texture components occurring in such steels

equation. Using the frictional form of the classical equation of motion with a strong damping term results in a steady state motion where the velocity of the defect depends only on the local force but not on its previous velocity. The overdamped steady state description is similar to choosing a linearized rate equation, where the defect velocity is described in terms of a temperature-dependent mobility term and the local driving pressure.

The calculation of the local forces in most vertex models is based on equilibrating the line energies of subgrain walls and large-angle grain boundaries at the interface junctions according to the Herring equation. The enforcement of the local mechanical equilibrium at these nodes is for obvious topological reasons usually only possible by allowing the abutting interfaces to curve.

These curvatures in turn act through their capillary force, which is directed towards the centre of curvature, on the junctions. In sum this may lead to their displacement. In order to avoid the artificial enforcement of a constant boundary curvature between two neighbouring nodes, the interfaces are usually decomposed into sequences of piecewise straight boundary segments.

Most vertex and network models use switching rules which describe the topological recombination of approaching vertices when such neighbouring nodes are closer than some critical spontaneous recombination spacing.. This is an analogy to the use of phenomenological annihilation and lock formation rules that appear in dislocation dynamics. As in all continuum models, the use of such empirical recombination laws replaces a more exact atomistic treatment.

It is worth noting in this context that the recombination rules, particularly the various critical recombination spacings, can affect the topological results of a simulation. Depending on the underlying constitutive continuum description, vertex simulations can consider crystal orientation and, hence, misorientations across the boundaries, interface mobility, and the difference in elastic energy between adjacent grains. Owing to the stereological complexity of grain boundary arrays and the large number of degrees of freedom encountered in such approaches, most network simulations are currently confined to the two-dimensional regime. The groups of Maurice and co-workers [**45**, **46**] and Kinderlehrer *et al.* [**50**, **51**] have also developed three-dimensional versions of the vertex approach.

Topological boundary dynamics models are different from kinetic cellular automaton or Potts Monte Carlo models in that they are not based on minimizing the total energy but directly calculate the motion of the lattice defects, usually on the basis of capillary and elastic forces. They are also different from phase field Ginzburg–Landau type interface models in that they use sharp rather than diffuse grain boundaries.

3 STATISTICAL MODELS FOR PREDICTING RECRYSTALLIZATION TEXTURES

3.1 The statistical microgrowth model of Sebald and Gottstein

The analytical formulation of physically based statistical models with a simple mathematical structure and at the same time solid metallurgical basis for fast applications in the area of process simulation remains an important challenge in materials science. This applies in particular for statistical recrystallization models which pursue the aim of predicting crystallographic texture, certain microstructure parameters (e.g. grain size), and even certain mechanical properties during processing with a precision which is sufficient for industrial applications.

In the past, various statistical Johnson–Mehl–Avrami–Kolmogorov (JMAK) approaches were suggested for the prediction of recrystallization textures. These models typically combine JMAK-type kinetic evolution equations with the texture dependence of grain nucleation and the misorientation dependence of the motion of grain boundaries. The most prominent and successful candidates of such orientation-dependent JMAK approaches for crystallographic texture prediction are the Bunge–Köhler [**52**] transformation model and the Sebald–Gottstein [**53**–**55**] kinetic model [**56**].

This concise review section on statistical texture models in the field of recrystallization is essentially inspired by these two formulations, particularly by the microgrowth selection Sebald–Gottstein model which is consistently formulated on the basis of nucleation and crystal growth kinetics while the Bunge–Köhler model essentially uses crystallographic transformations of the orientation distribution functions of the deformed samples without considering kinetics [**52**].

In the Sebald–Gottstein model the crystallographic texture of the deformed material is discretized in terms of a large set of discrete single orientations which approximate a given orientation distribution function of a plastically deformed specimen using typically cold-rolled sheet material.

Sebald and Gottstein investigated several nucleation mechanisms with respect to the orientation and misorientation distribution that they created at the incipient stages of recrystallization. The information that was provided by the submodels for nucleation are the orientation-dependent density of nuclei within the deformed crystals with a given crystallographic orientation. This means that the nucleation submodels initiate the orientation and misorientation distributions of the nuclei for primary recrystallization. The different types of nucleation process investigated by Sebald and Gottstein were random nucleation, creating both a random nucleus texture and a random misorientation distribution, nucleation at shear bands forming a random nucleus texture with a non-random misorientation distribution, and nucleation due to pre-existing nuclei, creating a nucleus texture similar to the deformation texture in conjunction with a narrow misorientation distribution.

The growth rate of the nuclei corresponds in the model to their grain boundary velocity which is given by the product of the grain boundary mobility and the local driving force. The mobility of a grain boundary depends on the misorientation between the growing and the deformed grain. Sebald and Gottstein distinguished three categories of grain boundaries, namely small-angle, large-angle, and special boundaries. Small-angle grain boundaries are assumed to be essentially immobile. In the case of aluminium it is generally accepted that grain boundaries with $40^\circ \langle 111 \rangle$ misorientation may show particularly high mobilities so that such interfaces are treated as special boundaries. This is realized in the simulations of Sebald and Gottstein by assigning higher mobilities to such grain boundaries. The mobility of an average large-angle grain boundary is typically set to 20 per cent of the maximum occurring mobility. The driving force for primary static recrystallization is the difference between the stored energy densities of the deformed matrix and the nucleus which in such models typically approximated in terms of the Taylor factor. Growth of the newly formed nuclei is assumed to be isotropic, but it ceases when the nuclei impinge. This means that a growing nucleus can only grow into the non-recrystallized volume fraction. This portion of the material can be calculated according to the JMAK theory which provides a relation between the increase in the recrystallized volume fraction for unconstrained growth (the so-called expanded volume fraction) and the true or constrained increase under consideration of grain impingement for a random spatial distribution.

In the Sebald–Gottstein model this relation is used to confine the growth of the nuclei to the non-recrystallized volume fraction. Details of the method and its mathematical formulation have been given in the original work of Sebald and Gottstein [**53**, **54**], Sebald [**55**], and Grumbach *et al.* [**56**].

When compared with the Potts, cellular automaton, or vertex models, statistical JMAK-type approaches such as those discussed above are more efficient for physically based recrystallization texture predictions

in the field of materials processing owing to their semistatistical formulation. On the other hand, statistical models neglect important local features of the microstructures such as the grain topology, the grain neighbourhood, and the local curvature of an interface. This can be a disadvantage when applying statistical models to heterogeneous microstructures.

3.2 A texture-component-based Avrami model

In this section a new texture-component-based JMAK model is described for the approximation of recrystallization textures. The approach is inspired by the Sebald–Gottstein microgrowth kinetic model. The method is based on the representation of both the deformation texture and the emerging recrystallization texture by a small set of discrete crystallographic Gauss-shaped texture components. These texture components are characterized in terms of their centre orientation, volume fraction, and scatter in orientation space. The main idea of the approach has two aspects. First, it reduces the number of deformed and newly formed recrystallized orientations to only a small number of discrete components. Second, it can make use either of a more physically based renormalization scheme or of an empirical fitting procedure to average the required activation energies from pairs of single orientations into corresponding equivalent values which are valid for pairs of texture components.

The main idea of using a small set of texture components instead of a large set of discrete single orientations consists in reducing the computational time required for the prediction of recrystallization textures and kinetics. Another advantage of this method is that the approach uses a small set of parameters which can be fitted from experiments.

Since each recrystallizing texture component can statistically interact with each deformation texture component, the kinetics are formulated as a tensorial variant of the JMAK kinetic equation. Each element of the kinetic tensor is derived from a set of two differential equations. The first equation describes the thermally activated nucleation and growth processes among the deformed and recrystallizing texture components for the expanded (unconstrained) volume fraction and the second equation is used for the correction to the true (constrained) volume fraction which accounts for impingement.

The respective driving forces, nucleation energies, and mobility coefficients between all different couples, each consisting of a recrystallizing and a deformed component to be swept, can be obtained from a geometrical renormalization procedure or from fitting. The method provides a very fast and efficient way to predict recrystallization textures phenomenologically on the basis of a physically based metallurgical approach.

The components which reproduce the deformation texture can be approximated from experimentally obtained pole figures or from single-orientation data sets. A fixed set of texture components which may occur as potential nucleation components is then defined which can be fitted from known typical recrystallization textures for the material investigated. For instance in the case of rolled body-centred cubic steels the most prominent potential recrystallization texture components are placed on or close to when the $\langle 111 \rangle$ direction is parallel to the normal direction (ND) of the sheet's texture fibre [**57**–**63**].

All nucleation texture components have the possibility to grow into all existing deformation texture components following their individual kinetics prescribed by the respective averaged activation energy for nucleation in a particular deformation component, the averaged mobility between the two texture components, and the driving force provided by the deformation component which is being swept. The kinetic parameters are hence essentially defined by the activation energy for nucleation, the activation energy for grain boundary mobility, and the stored energy in the various deformation texture components.

The kinetic parameters enter for each of the growing texture components, relative to the deformation components affected, a finite difference form of the JMAK kinetic equation under the assumption that the set of growing texture components sweeps the deformed texture components. The finite difference formulation has been earlier suggested by Sebald and Gottstein [**53**].

A challenge in that context is to identify the average values for the activation energy for nucleation, for the activation energy for grain boundary mobility, and for the stored deformation energy. This problem can be tackled via fitting to experimental data or by applying a renormalizing scheme as outlined in the following.

As described above, the texture component version of the texture-component JMAK model is based on the assumption that not many single discrete recrystallizing grains grow and mutually impede in another large set of single deformed matrix grains but that instead a small representative set of recrystallizing texture components grows into a small set of deformation texture components.

It is clear that is not likely to obtain by this approach a better insight into the physics of texture

formation during primary recrystallization than by the Sebald–Gottstein model or by spatially discrete models such as the Potts or cellular automaton approaches. Instead it is expected from such a coarse-graining procedure to render the analytical JMAK kinetic approach a powerful tool for fast and physically based process simulations of recrystallization texture evolution. The main new ingredient suggested here for expanding the JMAK kinetic theory along these lines, with the particular aim of making it more attractive for applications in the field of process modelling, lies in the introduction of a renormalization procedure for the transition from the growth of many single orientations to the growth of complete texture components considering both spatial and crystallographic aspects. This renormalization problem can be cast in a numerical or an analytical form.

The starting point of the procedure is the approach that a set of many single recrystallizing grains which have a similar crystallographic orientation and grow within a (homogeneous) deformed grain can be replaced by one single equivalent grain which is referred to as a recrystallizing texture component. This means that the multiple kinetics of the many similar expanding grains is replaced by a new equivalent texture component with a kinetic behaviour matching that of the group that it represents. This approach leads for each time interval to the formulation of an equivalent expanding volume which matches the sum over all individual volume changes during a certain time interval of the set of single grains which have an orientation that falls within a spherical Gaussian distribution function of the recrystallizing component and that grow during recrystallization into a certain deformed texture component. Under the assumption of certain boundary conditions this formulation can be used to extract an equivalent or renormalized activation term for the growth of that component.

Figures 7 and 8 show some exemplary results from this statistical texture-component-based simulation of primary static recrystallization of an IF steel at 900 °C. The subscript DEF indicates the volume fraction of the respective texture component in the deformed microstructure and the subscript RX indicates the volume fraction of the recrystallized texture component. The subscript DEF + RX indicates the complete volume fraction of the respective texture component summing up its fraction in the deformed and in the recrystallized state. In particular, the kinetics of the 45° ND rotated cube component is so slow that the simulated specimen does not undergo complete recrystallization after 200 s.

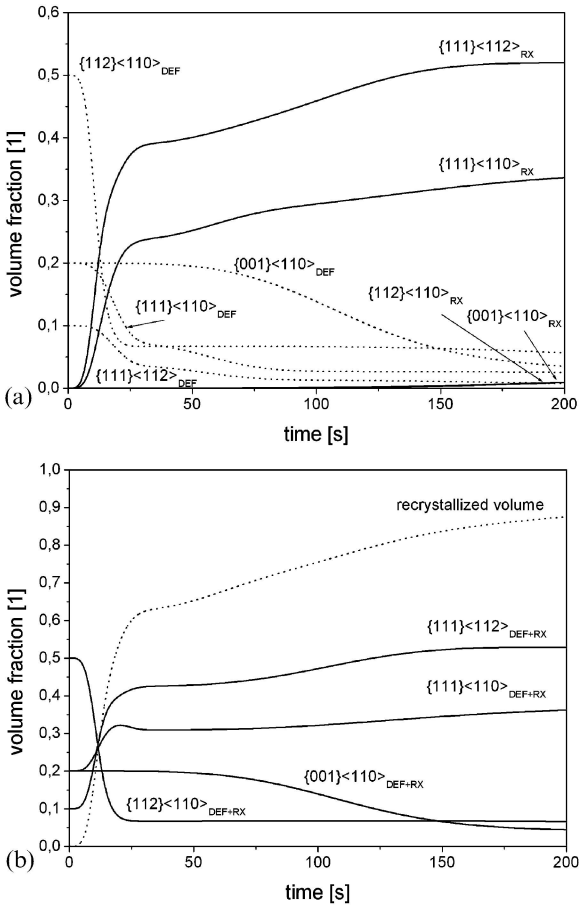

Fig. 7 Simulation by the use of a texture-component based Avrami model at 900 °C for a cold-rolled IF steel. The subscript DEF indicates the volume fraction of the respective texture component in the deformed microstructure; the subscript RX indicates the volume fraction of the respective texture component which is newly developed during primary static recrystallization; the subscript DEF + RX indicates the complete volume fraction of the respective texture component including its fraction in the deformed and in the recrystallized state

4 INPUT TO RECRYSTALLIZATION MODELS FOR TEXTURE PREDICTION

4.1 Incorporation of stored deformation energy into recrystallization models

Various approaches have been suggested to incorporate the stored deformation energy in recrystallization models for the prediction of crystallographic textures.

One important method lies in approximating the stored deformation energy from EBSD data [**29**, **64**]. In this method the Kikuchi pattern quality of the EBSD data is used with the aim of relating it to the

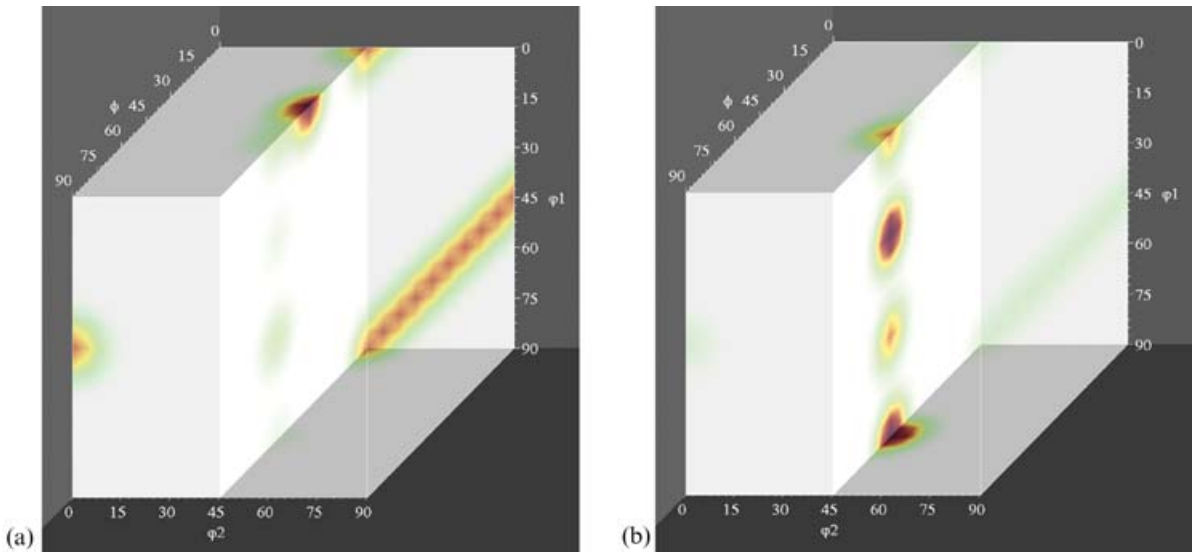

Fig. 8 Simulation at 900 °C for an IF steel (see the kinetics in Fig. 7), showing the orientation distribution functions; (a) starting texture of the deformed specimen; (b) texture of the simulated recrystallization texture after 200 s

stored dislocations density. The approach is based on the assumption that a high magnitude of the image quality corresponds to a small value of the stored deformation energy (Fig. 9).

A second common method lies in using the Taylor model. In this approach it is typically assumed that the stored deformation energy for each deformed grain with a given orientation can be related to the Taylor factor. The Taylor factor is the sum of the crystallographic shear for an imposed von Mises strain step as calculated via a polycrystal homogenization model. Two different approaches occur in current recrystallization models when using this method. One approach is based on the understanding that orientations which have a small Taylor factor correspond to areas with a high deformation potential, and thus to areas with a high stored deformation energy. An alternative view assumes that orientations which have a large Taylor factor correspond to areas with large accumulated strains, and thus to areas with a high stored deformation energy. In either case the Taylor approximation of the stored energy has two drawbacks. First, the method cannot properly capture the inhomogeneity of the deformation. Second, the Taylor factor alone only provides a measure of the current deformation state, but it does not consider the deformation history. It is likely, however, that the accumulation of the stored energy during a deformation path is determined not only by the final Taylor factor but by the path that the Taylor factor takes during grain rotation in the course of deformation.

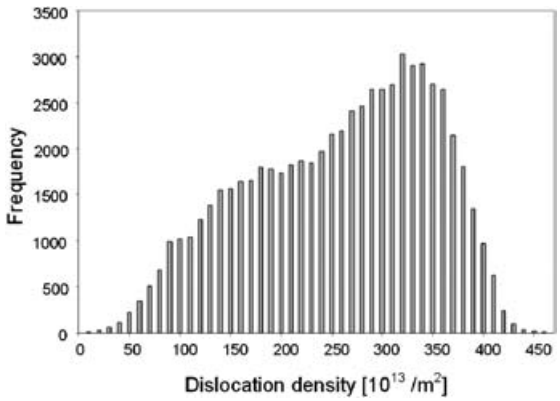

Fig. 9 Distribution of the dislocation density in a portion of a deformed steel sample as approximated from the Kikuchi pattern quality of its EBSD data. The maximum occurring dislocation density is equal to $47 \times 10^{14}\ \mathrm{m}^{-2}$ [**28**]

A third method for including the stored deformation energy into recrystallization models is based on the subgrain substructure. When assuming that the dislocation substructure can be described in form of subgrains with a given radius and a certain interface energy, the stored energy can be approximated as the sum of the entire inner surface energy.

A fourth and more direct approach for obtaining the stored deformation energy consists in extracting the stored deformation energy directly from a crystal plasticity finite element deformation provided that it uses a suitable constitutive model [**26**, **43**].

A fifth method for determining local values for the stored deformation energy consists in directly measuring local strains via digital image correlation photogrammetry on the grain scale [**65–67**].

4.2 Grain boundary input parameters into recrystallization models for texture prediction

Typically it is pertinent in recrystallization models to differentiate between small-angle grain boundaries which have a small mobility and large-angle grain boundaries which have a high mobility [**53–55**]. Additionally it makes sense to define certain special grain boundaries which may either have a very high or a very low mobility [**68–71**]. Typical examples are twin boundaries which have a very low mobility or highly mobile special grain boundaries such as the 40°, ⟨111⟩ grain boundaries in face-centred cubic metals or the 27°, ⟨110⟩ grain boundaries in body-centred cubic metals.

4.3 Grain nucelation

All recrystallization models presented above have in the past essentially been used as transformation models. This means that the primary recrystallization problem which consists of nucelation events (formation of mobile large-angle grain boundaries) on the one hand and growth events (expansion of grains into the deformation microstructure) on the other hand has been essentially reduced to solving the second step for a given nucelation spectrum. The actual study of nucleation mechanisms by conducting detailed and systematic simulations on the occurrence of discontinuous subgrain coarsening phenomena (in metals with a high stacking-fault energy such as aluminium) or nucleation events which work without discontinuous subgrain coarsening (in metals with a low stacking-fault energy such as austenitic stainless steels or brass) has been neglected in the past. Exceptions were the vertex simulations made by Humphreys [**40**, **41**] in that context which addressed the physics of nucleation events in subgrain-forming metals. It seems that the use of vertex models might be particularly promising for future research in that context since they can be used to discretize the local curvatures of unstressed subgrain structures in a very detailed fashion. An enormous obstacle on the other hand lies in statistics, since nucelation by discontinuous subgrain coarsening is a very rare event when normalized by the number of all subgrains in a deformed structure (high stacking-fault energy) from which one single nucleus emerges. Another difficulty lies in the three-dimensionality of the problem which is a time-consuming challenge in the field of vertex modelling.

Recently, abnormal subgrain growth has also been investigated as a nucleation mechanism for recrystallization by the use of Potts simulations by Holm *et al.* [**72**]. These workers used experimental input data on the microstructure, texture, and interface properties. Their results showed that abnormal growth events emerge spontaneously during evolution in metals with a high stacking-fault energy. It is particularly important that Holm *et al.* could link the occurrence of abnormal subgrain growth to mean field theory, i.e. the analysis predicted that the frequency of abnormal growth events was a function of local neighbourhood and the boundary misorientation distribution.

When using more statistical models which cannot map actual nucelation events, it is hence a practical alternative to anticipate certain nucleation mechanisms *a priori* and to assign a certain fraction to them [**73**, **74**].

5 CONCLUSIONS

A concise review was given of the most relevant models for predicting crystallographic textures that are formed during primary static recrystallization. The overview aimed at including approaches that are particularly suited to process modelling. Two groups of models were presented, namely those which spatially discretize the grains and the interface motion associated with recrystallization or subgrain coarsening respectively, and those which treat these phenomena in an Avrami-type statistical fashion. The first group included the Potts, cellular automaton, and vertex models. The second group included the Sebald–Gottstein model and a new texture-component-based JMAK approach. While the spatially discrete models pertaining to the first group include a larger number of details associated with individual grains (topology, neighbourhood, and local curvature) at the cost of larger calculation times, the models from the second group are much faster but less suitable when the materials described reveal heterogeneous microstructures. Finally the report ended with a concise review of the current status of the simulation of nucleation in the field of recrystallization modelling.

REFERENCES

1 **Humphries, F. J.** A unified theory of recovery, recrystallisation and grain growth, based on the stability and growth of cellular microstructures i, the basic model. *Acta Materialia*, 1997, **45**, 4231–4240.
2 **Doherty, R. D., Hughes, D. A., Humphreys, F. J., Jonas, J. J., Juul Jensen, D., Kassner, M. E., King, W. E., McNelley, T. R., McQueen, H. J.,** and

Rollett, A. D. Current issues in recrystallization: a review. *Mater. Sci. Engng* A, 1997, **238**, 219–274.
3 **Raabe, D.** *Computational materials science*, 1998 (Wiley–VCH, Weinheim).
4 **Smith, C. S.** Grains, phases and interfaces, an interpretation of microstructure. *Trans. AIME*, 1948, **175**, 15–51.
5 **Gottstein, G., Marx, V.,** and **Sebald, R.** Integral recrystallization modeling: from cellular automata to finite element analysis. In Proceedings of the Conference on *Recrystallization and related phenomena* (Eds T. Sakai and H. G. Suzuki), 1999, Vol. 13, pp. 15–24 (Japan Institute of Metals, Sendai).
6 **Raabe, D., Roters, F., Barlat, F.,** and **Chen, L.-Q.** (Eds) *Continuum scale simulation of engineering materials*, 2004 (Wiley–VCH).
7 **Humphreys, F. J.** and **Hatherly, M.** *Recrystallization and related annealing phenomena*, 1995, ch. 8, p. 235 (Pergamon, Oxford).
8 **Beck, P.** and **Hu, H.** In Proceedings of the ASM Seminar on *Recrystallization, grain growth and texture*, 1966 (American Society for Metals, Metals Park, Ohio).
9 **Haessner, F.** (Ed.) *Recrystallization*, 1978 (Dr Riederer Verlag, Stuttgart).
10 **Gottstein, G.** and **Sebald, R.** Thermomechanical processing of steel. In Proceedings of the J. J. Jones Symposium (Eds S. Yue and E. Essadiqi), 2000, pp. 21–45 (Canadian Institute of Mining, Metallurgy and Petroleum, Montreal, Quebec).
11 **Miodownik, M. A.** A review of microstructural computer models used to simulate grain growth and recrystallisation in aluminium alloys. *J. Light Metals*, 2002, **2**, 125–135.
12 **von Neumann, J.** *Collected works of John von Neumann* (Vol. Ed. A. W. Burks), Vol. 5, 1963 (Pergamon, Oxford).
13 **Hesselbarth, H. W.** and **Göbel, I. R.** Simulation of recrystallization by cellular automata. *Acta Metallurgica*, 1991, **39**, 2135–2144.
14 **Pezzee, C. E.** and **Dunand, D. C.** The impingement effect of an inert, immobile second phase on the recrystallization of a matrix. *Acta Metallurgica*, 1994, **42**, 1509–1522.
15 **Sheldon, R. K.** and **Dunand, D. C.** Computer modeling of particle pushing and clustering during matrix crystallization. *Acta Materialia*, 1996, **44**, 4571–4582.
16 **Davies, C. H. J.** The effect of neighbourhood on the kinetics of a cellular automaton recrystallisation model. *Scripta Metallurgica et Materialia*, 1995, **33**, 1139–1154.
17 **Marx, V., Raabe, D.,** and **Gottstein, G.** Simulation of the influence of recovery on the texture development in cold rolled BCC-alloys during annealing. In Proceedings of the 16th Risø International Symposium on *Materials science: materials: microstructural and crystallographic aspects of recrystallization* (Eds N. Hansen, D. Juul Jensen, Y. L. Liu, and B. Ralph), 1995, pp. 461–466 (Risø National Laboratory, Risø, Roskilde).
18 **Marx, V., Raabe, D., Engler, O.,** and **Gottstein, G.** Simulation of the texture evolution during annealing of cold rolled bcc and fcc metals using a cellular automaton approach. *Textures Microstructs*, 1997, **28**, 211–218.
19 **Marx, V., Reher, F. R.,** and **Gottstein, G.** Stimulation of primary recrystallization using a modified three-dimensional cellular automaton. *Acta Materialia*, 1998, **47**, 1219–1230.
20 **Davies, C. H. J.** Growth of nuclei in a cellular automaton simulation of recrystallisation. *Scripta Materialia*, 1997, **36**, 35–46.
21 **Davies, C. H. J.** and **Hong, L.** Cellular automaton simulation of static recrystallization in cold-rolled AA1050. *Scripta Materialia*, 1999, **40**, 1145–1152.
22 **Raabe, D.** Introduction of a scaleable 3D cellular automaton with a probabilistic switching rule for the discrete mesoscale simulation of recrystallization phenomena. *Phil. Mag. A*, 1999, **79**, 2339–2358.
23 **Raabe, D.** Cellular automata in materials science with particular reference to recrystallization simulation. *A. Rev. Mater. Res.*, 2002, **32**, 53–76.
24 **Raabe, D.** Mesoscale simulation of recrystallization textures and microstructures. *Adv. Engng Mater.*, 2001, **3**, 745–752.
25 **Janssens, K. G. F.** Random grid, three-dimensional, space-time coupled cellular automata for the simulation of recrystallization and grain growth. *Modelling Simulation Mater. Sci. Engng*, 2003, **11**, 157.
26 **Raabe, D.** and **Becker, R.** Coupling of a crystal plasticity finite element model with a probabilistic cellular automaton for simulating primary static recrystallization in aluminum. *Modelling Simulation Mater. Sci. Engng*, 2000, **8**, 445–462.
27 **Raabe, D.** Yield surface simulation for partially recrystallized aluminum polycrystals on the basis of spatially discrete data. *Comput. Mater. Sci.*, 2000, **19**, 13–26.
28 **Raabe, D., Roters, F.,** and **Marx, V.** Experimental investigation and numerical simulation of the correlation of recovery and texture in bcc metals and alloys. *Textures Microstructs*, 1996, **26–27**, 611–635.
29 **Raabe, D.** and **Hantcherli, L.** 2D cellular automaton simulation of the recrystallization texture of an IF sheet steel under consideration of Zener pinning. *Comput. Mater. Sci.*, 2005, **34**, 299–313.
30 **Srolovitz, D. J., Grest, G. S.,** and **Anderson, M. P.** Computer simulation of recrystallization – I. Homogeneous nucleation and growth. *Acta Metallurgica*, 1986, **34**, 1833–1845.
31 **Doherty, R. D., Srolovitz, D. J., Rollet, A. D.,** and **Anderson, M. P.** On the volume fraction dependence of particle limited grain growth. *Scripta Metallurgica*, 1987, **21**, 675–679.
32 **Rollett, D., Srolovitz, D. J., Anderson, M. P.,** and **Doherty, R. D.** Computer simulation of recrystallization – III. Influence of a dispersion of fine particles. *Acta Metallurgica*, 1992, **40**, 3475–3495.
33 **Raabe, D.** Scaling of Monte Carlo Kinetics of the Potts model using rate theory. *Acta Materialia*, 2000, **48**, 1617–1628.

34 **Holm, E. A.** and **Battaile, C. C.** The computer simulation of microstructural evolution. *J. Metals*, 2001, **53**(9), 20–23.

35 **Rollett, A. D.** and **Raabe, D.** A hybrid model for mesoscopic simulation of recrystallization. *Comput. Mater. Sci.*, 2001, **21**, 69–78.

36 **Radhakrishnan, B., Sarma, G., Weiland, H.,** and **Baggethun, P.** Simulations of deformation and recrystallization of single crystals of aluminum containing hard particles. *Modelling Simulation Mater. Sci. Engng*, 2000, **8**, 737–750.

37 **Thomas, I.** PhD Dissertation Thesis, Max-Planck-Institut für Eisenforschung, 2006 (in preparation).

38 **Zaefferer, S.** Application of orientation microscopy in SEM and TEM for the study of texture formation during recrystallisation processes. In Proceedings of the 14th International Conference on Textures of Materials (*ICOTOM 14*), Leuven, Belgium, 2005, in *Mater. Sci. Forum*, 2005, **495–497**, 3–12.

39 **Thomas, I., Zaefferer, S., Friedel, F.,** and **Raabe, D.** Concepts for integrating plastic anisotropy into metal forming simulations. *Advd Engng Mater.*, 2003, **5**(8), 566–570.

40 **Humphreys, F. J.** Modeling mechanisms and microstructures of recrystallisation. *Mater. Sci. Technol.*, 1992, **8**, 135–143.

41 **Humphreys, F. J.** A network model for recovery and recrystallisation. *Scripta Metallurgica*, 1992, **27**, 1557–1562.

42 **Svoboda, J.** Comment on Humphreys' paper 'A network model for recovery and recrystallisation'. *Scripta Metallurgica*, 1996, **28**, 1589–1590.

43 **Bate, P.** Modelling deformation microstructure with the crystal plasticity finite-element method. *Phil. Trans. R. Soc. Lond. A*, 1999, **357**, 1589–1601.

44 **Bate, P.** 2- and 3-D curvature driven vertex simulations of grain growth. In Proceedings of the First Joint International Conference on *Recrystallization and grain growth*, 2001, Vol. 1, pp. 39–48 (Springer-Verlag, Berlin).

45 **Maurice, C.** and **Humphries, J.** 2- and 3-D curvature driven vertex simulations of grain growth. In *Grain growth in polycrystalline materials III*, 1998, Vol. 1, pp. 81–90 (Minerals, Metals and Materials Society, Warrendale, Pennsylvania).

46 **Maurice, C.** 2- and 3-D curvature driven vertex simulations of grain growth. In Proceedings of the First Joint International Conference on *Recrystallization and grain growth*, 2001, Vol. 1, pp. 123–134 (Springer-Verlag, Berlin).

47 **Weygand, D., Brechet, Y.,** and **Lepinoux, J.** A vertex simulation of grain growth in 2D and 3D. *Advd Engng. Mater*, 2001, **3**, 67–71.

48 **Prangnell, P. B., Hayes, J. S., Bowen, J. R., Apps, P. J.,** and **Bate, P. S.** Continuous recrystallisation of lamellar deformation structures produced by severe deformation. *Acta Materialia*, 2004, **52**, 3193–3206.

49 **Weygand, D., Brechet, Y.,** and **Lepinoux, J.** Zener pinning and grain growth: a two-dimensional vertex computer simulation. *Acta Materialia*, 1999, **47**, 961–970.

50 **Kinderlehrer, D., Livshits, I., Rohrer, G. S., Ta'asan, S.,** and **Yu, P.** Mesoscale evolution of the grain boundary character distribution. In Proceedings of the Conference on Recrystallization and Grain Growth, in *Mater. Sci. Forum*, 2004, **467–470**, 1063–1068.

51 **Kinderlehrer, D., Livshits, I., Manolache, F., Rollett, A. D.,** and **Ta'asan, S.** An approach to the mesoscale simulation of grain growth. Influences of interface and dislocation behavior on microstructure evolution. *Mater. Res. Soc. Symp. Proc.*, 2001, **652**, Y1.5.

52 **Bunge, H. J.** and **Köhler, U.** Model calculations of primary recrystallization textures. *Scripta Metallurgica Materialia*, 1992, **27**, 1539–1543.

53 **Sebald, R.** and **Gottstein, G.** Modeling of recrystallization textures: interaction of nucleation and growth. *Acta Materialia*, 2002, **50**, 1587–1598.

54 **Sebald, R.** and **Gottstein, G.** Simulation of textural evolution during primary static recrystallization. In Proceedings of the 12th International Conference on *The textures of materials* (*ICOTOM 12*), Montreal, Quebec, Canada, 1999, Vol. 1, p. 292 (NCR Research Press, Otawa, Ontario).

55 **Sebald, R.** *Modellierung der Rekristallisationstextur: Wechselwirkung zwischen Keimbildung und Keimwachstum*. PhD Dissertation, Rheinisch–Westfälish Technische Hochschule, Aachen, Germany, 2001.

56 **Crumbach, M., Goerdeler, M.,** and **Gottstein, G.** Modelling of recrystallisation textures in aluminium alloys: I. Model set-up and integration. *Acta Materialia*, 2006, **54**(12), 3275–3289.

57 **Hölscher, M., Raabe, D.,** and **Lücke, K.** Rolling and recrystallization textures of bcc steels. *Steel Res.*, 1991, **62**, 567–575.

58 **Ushioda, K., von Schlippenbach, U.,** and **Hutchinson, W. B.** The effect of carbon content on recrystallisation and texture development in steel. *Textures Microstructs*, 1987, **7**, 11–28.

59 **Raabe, D.** and **Lücke, K.** Textures of ferritic stainless steels. *Mater. Sci. Technol.*, 1993, **9**, 302–312.

60 **Raabe, D.** and **Lücke, K.** Annealing textures of bcc metals. *Scripta Metallurgica Materialia*, 1992, **27**, 1533–1538.

61 **Klinkenberg, C., Raabe, D.,** and **Lücke, K.** Influence of volume fraction and dispersion rate of grain boundary cementite on the cold rolling textures of low carbon steels. *Steel Res.*, 1992, **63**, 227–276.

62 **Raabe, D.** Investigation of the orientation dependence of recovery in low-carbon steel by use of single orientation determination. *Steel Res.*, 1995, **66**, 222–229.

63 **Juntunen, P., Raabe, D., Karjalainen, P., Kopio, T.,** and **Bolle, G.** Optimizing continuous annealing of IF steels for improving their deep drawability. *Metall. Mater. Trans. A*, 2001, **32**, 1989–1995.

64 **Choi, S.-H.** Simulation of stored energy and orientation gradients in cold-rolled interstitial free steels. *Acta Mater.*, 2003, **51**, 1775–1788.

65 **Raabe, D., Sachtleber, M., Zhao, Z., Roters, F.,** and **Zaefferer, S.** Micromechanical and macromechanical

effects in grain scale polycrystal plasticity experimentation and simulation. *Acta Materialia*, 2001, **49**, 3433–3451.

66 Kuo, J.-C., Zaefferer, S., Zhao, Z., Winning, M., and **Raabe, D.** Deformation behaviour of aluminium bicrystals. *Advd Engng Mater.*, 2003, **5**(8), 563–566.

67 Zaefferer, S., Kuo, J.-C., Zhao, Z., Winning, M., and **Raabe, D.** On the influence of the grain boundary misorientation on the plastic deformation of aluminum bicrystals. *Acta Materialia*, 2003, **51**, 4719–4735.

68 Gottstein, G. and **Shvindlerman, L. S.** *Grain boundary migration in metals – thermodynamics, kinetics, applications*, 1999 (CRC Press, Boca Raton, Florida).

69 Shvindlerman, L. S. and **Gottstein, G.** Grain boundary and triple junction migration – the latest advances. In Proceedings of the Conference on *Recrystallization and related phenomena* (Eds T. Sakai and H. G. Suzuki), 1999, Vol. 13, pp. 431–438 (Japan Institute of Metals, Sendai).

70 Upmanyu, M., Srolovitz, D. J., Shvindlerman, L. S., and **Gottstein, G.** Misorientation dependence of intrinsic grain boundary mobility: simulation and experiment. *Acta Materialia*, 1999, **47**, 3901–3914.

71 Furtkamp, M., Gottstein, G., Molodov, D. A., Semenov, V. N., and **Shvindlerman, L. S.** Grain boundary migration in Fe3.5%Si bicrystals with ⟨001⟩ tilt boundaries. *Acta Materialia*, 1998, **46**, 4103–4110.

72 Holm, E. A., Miodownik, M. A., and **Rollett, A. D.** On abnormal subgrain growth and the origin of recrystallization nuclei. *Acta Materialia*, 2003, **51**, 2701–2716.

73 Engler, O., Vatne, H. E., and **Nes, E.** The roles of oriented nucleation and oriented growth on recrystallization textures in commercial purity aluminium. *Mater. Sci. Engng A*, 1996, **205**, 187–198.

74 Engler, O. Influence of particle stimulated nucleation on the recrystallization textures in cold deformed Al-alloys. Part II – modeling of recrystallization textures. *Scripta Materialia*, 1997, **37**, 1675–1683.